Association Phenomena of Poly(acrylic acid)-*b*-poly(2-vinylpyridine)-*b*-poly(acrylic acid) Triblock Polyampholyte in Aqueous Solutions: From Transient Network to Compact Micelles

Vasiliki Sfika and Constantinos Tsitsilianis*

Department of Chemical Engineering, University of Patras, 26500 Patras, Greece, and Institute of Chemical Engineering and High-Temperature Chemical Processes, FORTH-ICE/HT, P.O.Box 1414, 26500 Patras, Greece

Received January 6, 2003; Revised Manuscript Received April 16, 2003

ABSTRACT: An asymmetric model triblock copolymer of poly(acrylic acid)-*b*-poly(vinylpyridine)-*b*-poly(acrylic acid) (PAA-*b*-P2VP-*b*-PAA) was synthesized through anionic polymerization and explored in aqueous media. This block polyampholyte exhibits a rich phase behavior responding to pH changes. At low pH and low concentrations the polymer is molecularly dissolved. At pH close to 3.4 and above a critical concentration, a three-dimensional transient network is formed. The physical cross-links arise from electrostatic interactions among protonated positively charged P2VP units and negatively charged PAA units. In the intermediate pH region ($4 < pH < 7$) and around the isoelectric point, the polyampholyte is precipitated. The polymer is redissolved at higher pH, forming compact micelles with P2VP hydrophobic cores and extended PAA chains in the corona. The phase behavior of the system is reversible.

Introduction

It is well-known that amphiphilic block copolymers (e.g., bearing hydrophilic and hydrophobic blocks) undergo association through hydrophobic interactions forming micellar nanostructures and/or physical networks in aqueous solutions. The properties of the so-formed self-assemblies depend on the copolymer architecture and the nature, mainly, of the hydrophilic part of the copolymer. The ability of ionization of the soluble chains has fundamental consequences on the behavior of the copolymer. Polymeric systems that respond to environmental stimuli such as pH and ionic strength have been the subject of increasing interest because of their potential applications in drug delivery systems, and water-born coatings.

Much work has been devoted to the study of diblock copolymers constituted of a hydrophobic block and a hydrophilic weak polyelectrolyte block either anionic or cationic. An interesting category of such systems are those containing a poly(2-vinylpyridine) (P2VP) block which can be protonated and therefore can become water-soluble at low pH. Spherical micelles formed in water by P2VP−PtBA (poly(*tert*-butyl acrylate) diblock copolymers are sensitive to pH and ionic strength of the solution since their size is controlled by the degree of stretching of the micellar shells.[1]

pH-induced micellization takes place when the block-partner of P2VP is a water-soluble nonionic polymer such as poly(ethylene oxide) (PEO). These copolymers exhibit a fully reversible pH-dependent micellization. At pH higher than 5 P2VP is deprotonated and becomes hydrophobic. Stable micelles are then formed with a P2VP core and PEO corona.[2]

P2VP has also been combined with weak polyelectrolytes, either anionic or cationic, in block copolymers. Recently Jerome et al. have studied the associative behavior of poly(2-vinylpyridine)-*b*-poly[2-(dimethylamino)ethyl methacrylate] diblock copolymers in aqueous systems as a function of pH, ionic strength, and temperature. The difference between the p*K*s of the two basic blocks is the reason these block copolymers exhibit an interesting aggregation behavior.[3]

Poly(vinylpyridine)-*b*-poly(acrylic acid) has been studied as a desalination membranes. These copolymers containing ionizable weak acid and weak basic blocks, can lead to a polyampholytic system in a certain range of pH.[4]

Other diblock polyampholytes have been designed and investigated in aqueous systems as a function of pH.[5] The macromolecular architecture has been recognized as a very important factor affecting the solution properties of copolymers. In this context, ABC triblock copolymers combining a hydrophobic block a polyacid and a polybase have been synthesized by "living" polymerization techniques and studied in aqueous solutions.[6] Although ABC triblock polyampholytes have only recently started to be investigated, simpler triblock polyampholytes of the ABA type are still unexplored.

In this work, a model poly(acrylic acid)−poly(2-vinylpyridine)−poly(acrylic acid) block polyampholyte with a relatively long P2VP middle block end-capped with short PAA blocks was synthesized by anionic polymerization and investigated in aqueous solutions as a function of pH. Association phenomena leading to the formation of micelles and/or to physical gels in different pH regimes will be demonstrated and discussed.

Experimental Part

Materials. Tetrahydrofuran (THF) free from protonic impurities was obtained according to standard procedures. 2-Vinylpyridine (2VP) (Merck) was distilled over sodium wire under vacuum, then dried overnight over calcium hydride (CaH_2), and vacuum distilled into burets before the synthesis. *tert*-Butyl acrylate (tBA) (Merck) was first vacuum distilled from

* To whom correspondence should be addressed at the University of Patras.

10.1021/ma0300084 CCC: $25.00
Published on Web 06/06/2003

CaH_2 and then treated with triethyl aluminum (Aldrich, 1 M solution in heptane). Once a faint yellow color obtained, tBA was immediately distilled into burets. Sodium tetraphenyldiisobutane was prepared by the reaction of Na metal chips with diphenyl ethylene (Merck), in tetrahydrofuran. The initiator was titrated with acetanilide prior to use.

Synthesis. The precursor copolymer poly(*tert*-butyl acrylate)−poly(2-vinylpyridine)−poly(*tert*-butyl acrylate) (PtBA−P2VP−PtBA) was synthesized by anionic polymerization, in a glass reactor, under an argon atmosphere, in THF. 2VP was first polymerized, at −75 °C, using the bifunctional initiator sodium tetraphenyldiisobutane to provide chain growth at both ends of the macromolecule. Prior the addition of the second monomer a sample was taken from the reaction media, for the purpose of characterization. Then, the second monomer tBA was added dropwise at −65 °C. A sudden color change from dark red to pale yellow confirmed the rapid and quantitative initiation of the polymerization of the second monomer. The polymerization was terminated by the addition of a small amount of methanol.

Hydrolysis. The (PtBA−P2VP−PtBA) precursor copolymer was subjected to acid hydrolysis with a 5-fold molar excess of concentrated HCl, in 1,4-dioxane at 80 °C for 12 h. The hydrolysis degree of the copolymer was determined by ^{1}H NMR in a mixture of deuterated MeOH:$CDCl_3$ (3:1) and also by potentiometric titration using 0.1 N NaOH.

Size Exclusion Chromatography. SEC of the P2VP and PtBA−P2VP−PtBA precursor macromolecules were carried out using a set of three μ-Styragel columns of 10^3, 10^4, and 10^5 Å porosity and a differential refractometer as detector (model ERC-7515, ERC Inc.). The mobile phase was a 2% triethylamine solution in tetrahydrofuran and the flow rate 1 mL min^{-1}. The calibration curve was obtained by PS standards.

Static Light Scattering. All the light-scattering experiments were carried out using a thermally regulated (±0.1 °C) spectrogoniometer, model SEM RD (Sematech France), equipped with a He−Ne laser (633 nm). The refractive index increments d*n*/d*c* required for the interpretation of the static light scattering measurements were determined using a Chromatic KMX-16 differential refractometer operating at 633 nm. The dynamic light scattering measurements were performed using a R.T.G. correlator (Sematech France). The correlation functions were analyzed to the second order by the method of cumulants, the pinhole was 200 nm, and the scattering angle was 90°.

Rheology. Rheological measurements were performed at 25 °C on a controlled stress rheometer (Rheometrics SR-200) using a cone/plate geometry (diameter 40 mm). After loading of the samples, a rest period of 5 min was applied, to erase any shear history effects. The shear stress ramping used to collect the data was 0.3 Pa/s.

ζ-Potential. ζ-potential measurements were carried out at 25 °C, using a Zetaseizer 5000 (Malvern Instruments Ltd.) equipped with a cell type ZET 5104 (cross beam mode).

Turbidity. Turbidity measurements were carried out operating at 490 nm, using a U-2001 Hitachi spectrophotometer, at 25 °C.

Potentiometric Titration. Potentiometric titration was performed using a digital pH-meter 751 GPD Titrino (Metrohm), at 25 °C.

NMR. ^{1}H NMR spectra were measured on a Bruker AC-200 spectrometer, at room temperature, in $CDCl_3$ or deuterated methanol.

Viscometry. Viscometric measurements were carried out using a Shott AVS-300 automated system, using Ostwald-type capillary viscometers in a thermally regulated water bath at 25 °C.

Results and Discussion

Synthesis and Characterization. A three-step synthetic procedure was followed to prepare the PAA−P2VP−PAA triblock polyampholyte (Scheme 1). In the first and second steps, a PtBA−P2VP−PtBA block copolymer was synthesized by "living" anionic polymerization using a bifunctional initiator and sequential addition of the monomers. 2VP was polymerized first by using sodium tetraphenyldiisobutane as the initiator at −75 °C. After the consumption of the monomer, a small amount was sampled out, and the tBA was added and allowed to be polymerized at −65 °C. To ensure "living" conditions for the 2VP and tBA polymerization, a 5-fold LiCl molar excess with respect to the initiator was present in the medium.[7] The reaction was terminated with methanol, and the polymer was precipitated in heptane, redissolved in benzene, filtered, and freeze-dried.

Scheme 1

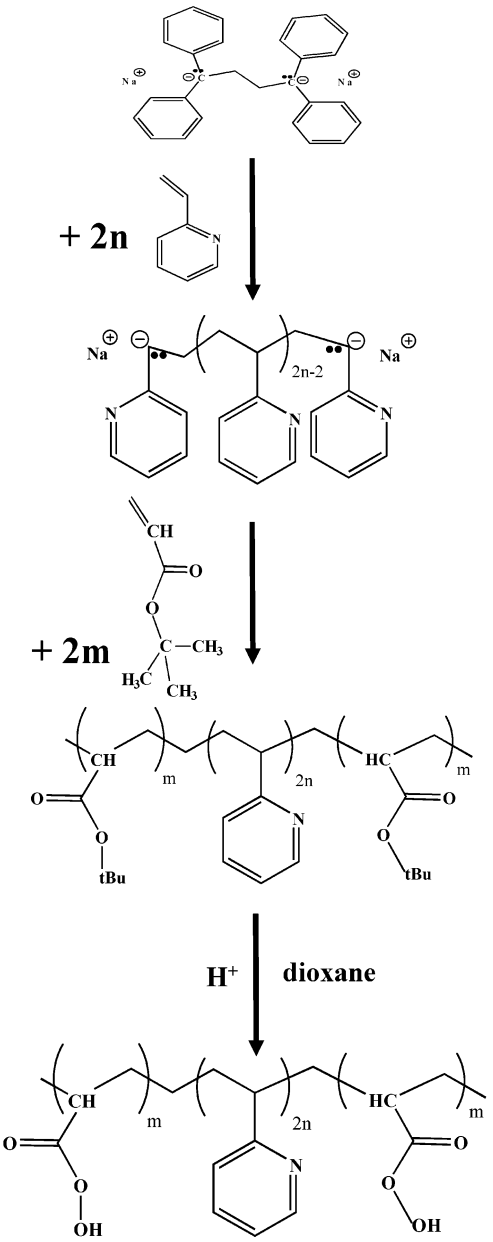

Size exclusion chromatograms of the P2VP precursor and the PtBA−P2VP−PtBA triblock copolymers are shown in Figure 1. As can be seen, there is no trace of homo-P2VP in the raw final product, confirming the absence of accidentally deactivated P2VP impurities. The PtBA−P2VP−PtBA exhibits narrow molecular polydispersity. Diblock P2VP−PtBA impurities arising

Table 1. Molecular Characteristics of the ABA Polyampholyte

	M_w/M_n[a]	wt %[b]		M_w	
P2VP	1.11			66 000[c]	$P2VP_{628}$
PtBA−P2VP−PtBA	1.11	P2VP	65.7	100 000[d]	$PtBA_{134}-P2VP_{628}-PtBA_{134}$
		PtBA	34.3		
PAA−P2VP−PAA		P2VP	76.4	85 000[d]	$PAA_{134}-P2VP_{628}-PAA_{134}$
		PAA	20.95	62 500[e]	
		PtBA	2.65		

[a] Measured by GPC. [b] Measured by NMR. [c] Measured by static light scattering in THF. [d] Calculated by the M_w of the precursor P2VP and the composition. [e] Apparent M_w, measured by static light scattering in H_2O, pH = 3.4.

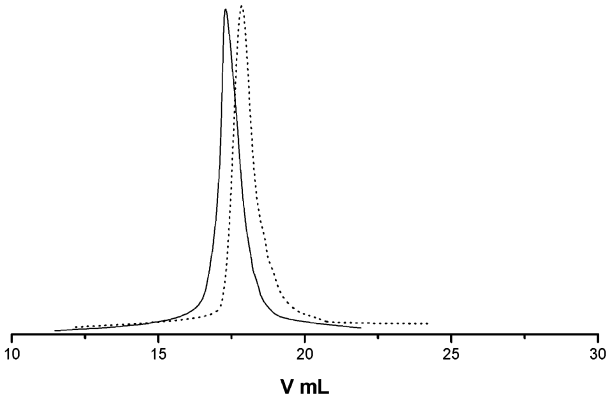

Figure 1. SEC chromatograms of the $PAA_{134}-P2VP_{628}-PAA_{134}$ triblock copolymer (−) and its P2VP (···) precursor.

from deactivation of one of the two P2VP anions is not detectable by SEC.

Static light scattering and ^1H NMR was further employed to characterize the molecular weight and the composition of the copolymer, the molecular features of which are shown in Table 1.

In the third step, the PtBA−P2VP−PtBA precursor was subjected to acid-catalyzed hydrolysis in dioxane at 80 °C in order to modify the PtBA end-blocks to poly(acrylic acid), PAA. The obtained PAA−P2VP−PAA copolymer was finally dissolved in water and was purified by dialysis and freeze-dried. The degree of hydrolysis of the copolymer was determined by ^1H NMR and potentiometric titration and was found to be 95% and 93.3%, respectively. Hereafter the final product will be designated as $PAA_{134}-P2VP_{628}-PAA_{134}$, and its characteristics are presented in Table 1.

pH-Dependent Solution Properties. The copolymer, composed of P2VP and PAA blocks, is expected to exhibit the characteristics of a polyampholyte since P2VP can protonated at low pH, behaving as a weak base, while the PAA is charged at high pH, behaving as a weak acid.

The copolymer is soluble in water after dialysis. Dilute aqueous solutions are clear giving a pH close to 3.4. Then the copolymer was titrated by NaOH. The potentiometric titration curve of 0.1 wt % polymer is shown in Figure 2. Because of the relative proximity of the effective p*K*s of the P2VP and PAA, the titration curve does not present two distinct inflections corresponding to the different p*K*s of the constituents but rather a continuous titration of the acidic units. This behavior imposes a difficulty in assigning the deprotonation order. However the deprotonation of the $2VPH^+$ moieties is expected to be more favorable (lower p*K*) occurring first.

To determine the isoelectric point (iep) of the $PAA_{134}-P2VP_{628}-PAA_{134}$ polyampholyte (the PAA/P2VP molar ratio is 0.42), turbidimetric titration and electrophoresis

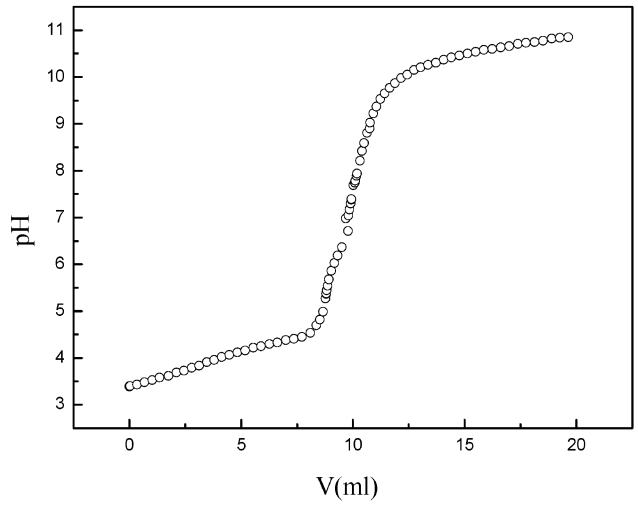

Figure 2. Hydrogen ion titration curve of the $PAA_{134}-P2VP_{628}-PAA_{134}$ in water (1 mg/mL) with 0.01 N NaOH.

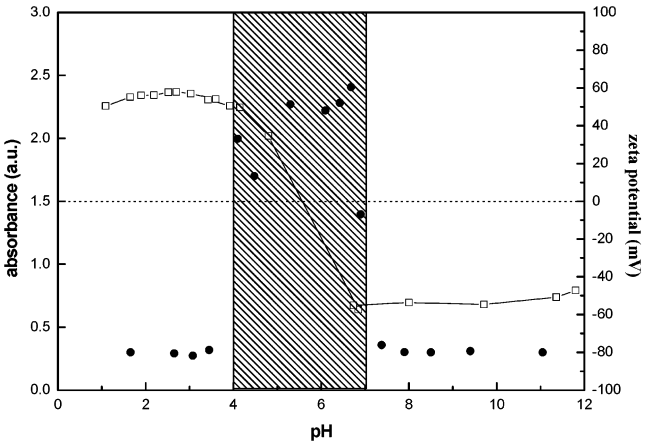

Figure 3. Variation of optical density (●) and ζ-potential (□) as a function of pH for $PAA_{134}-P2VP_{628}-PAA_{134}$ 0.2 wt % aqueous solution at 25 °C.

measurements have been performed. In Figure 3, the optical density of a 0.2 wt % copolymer solution is plotted as a function of pH. At pH higher than 4, the solution turns turbid and the copolymer precipitates, leading to a milky dispersion prevented from precipitation by stirring. At pH higher than 7, the copolymer again becomes soluble, leading to a clear solution. Precipitation of polyampholytes in the isoelastic region depends on whether the predominant species exist as polyzwitterions or uncharged groups.[8] Our system belong to the second case, and the observed precipitation is due to the similarity of the p*K*s of the P2VP, PAA sequences. Therefore, the iep can be approximately estimated at pH 5.5, corresponding to the midpoint of the precipitation region.

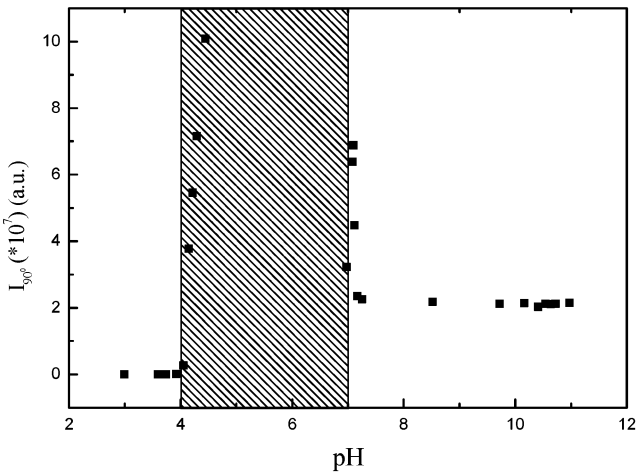

Figure 4. Variation of the light-scattered intensity at 90° angle, I_{90}, as a function of pH for a $PAA_{134}-P2VP_{628}-PAA_{134}$ aqueous solution (0.1 wt %) at 25 °C.

In Figure 3, the ζ-potential of the solution is also depicted as a function of pH. As can be seen the copolymer has an iep approximately at pH 5.5 in accordance with the turbidimetric measurements. The iep values estimated by the two methods are in good agreement with the theoretical value 5.7 calculated from the polyampholyte composition and the effective p*K*s of the corresponding P2VP and PAA homopolymer blocks.[9]

From Figure 3, three pH regions can be distinguished: the low pH region, pH < 4, the intermediate precipitation region and the high pH region, pH > 7. Further exploration of the pH-dependent solution behavior of the system was conducted by static light scattering. In Figure 4, the intensity of the light scattered at an angle of 90°, I_{90}, of a 0.1 wt % polymer solution is presented as a function of pH. In the low pH region, I_{90} is weak, demonstrating that in low concentrations association phenomena may be absent. On the contrary, in the high pH region, the scattered intensity is strong, revealing that aggregation phenomena take place. In this pH region, the P2VP middle block is entirely deprotonated, becoming hydrophobic. The polyampholyte is turned to an amphiphilic block copolymer, and micellization phenomena are expected to occur.

Additional information can be obtained from the pH-dependence viscosity. In Figure 5, the reduced viscosity, η_{sp}/c, for $c = 0.2$ wt % is plotted as a function of pH. The system exhibits a rich viscometric behavior. In the low pH region, a pronounced and sharp maximum appears while in the high pH region, the reduced viscosity is considerably lower passing through a shallow maximum at elevated pH. The latter is consistent with the light scattering data of Figure 4, showing that compact micellar structures are formed.

The High pH Region. To determine the characteristics of the micelles in the high pH region, static and dynamic light scatterings were carried out in water by using solutions at pH close to 11. In Figure 6, the concentration dependence of the inverse scattering intensity extrapolated to zero angle, $(Kc/\Delta I)_{\theta=0}$ of $PAA_{134}-P2VP_{628}-PAA_{134}$ where K is the optical constant and ΔI the scattering intensity difference between the solution and the solvent, is depicted. From the linear part of the curve, where polymolecular micelles dominate, the apparent values of the molecular weight ($M_w = 4.7 \times 10^6$ g mol^{-1}) and the radius of gyration ($R_g =$ 53 nm) of the micelles were determined. The aggregation number is estimated to be 55 and is independent of pH at this regime as can be observed in Figure 4.

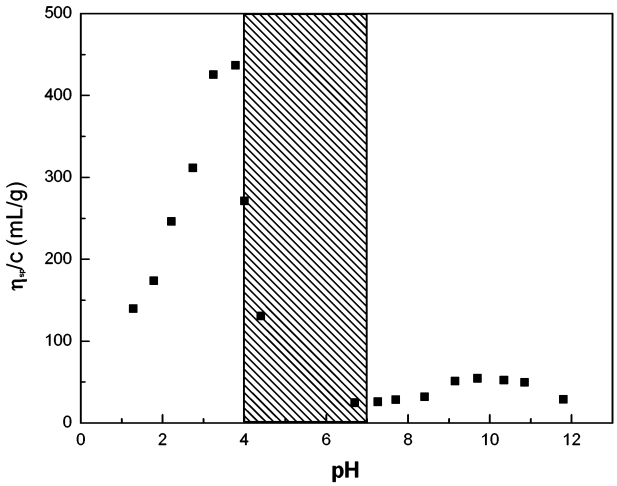

Figure 5. Variation of the reduced viscosity, η_{sp}/c, as a function of pH for a $PAA_{134}-P2VP_{628}-PAA_{134}$ aqueous solution (0.2 wt %) at 25 °C.

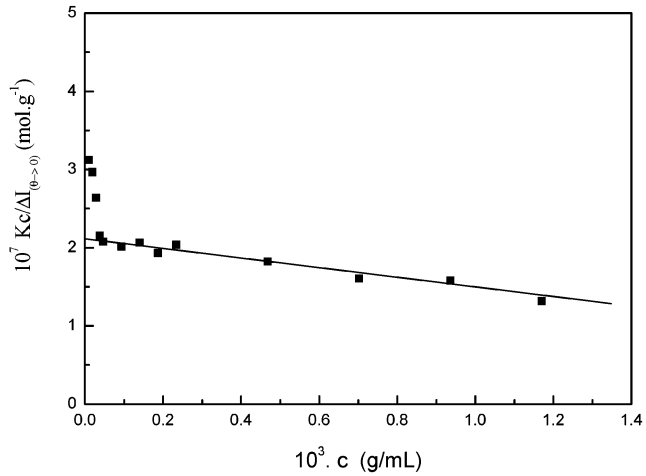

Figure 6. Concentration dependence of the reduced viscosity, η_{sp}/c, for the $PAA_{134}-P2VP_{628}-PAA_{134}$ in water at pH 3.4 and 25 °C.

The hydrodynamic radius R_H of the micelles is 37 nm, as determined according to the Stokes−Einstein equation

$$R_H = \frac{k_B T}{6\pi\eta_o D_o} \quad (1)$$

where k_B is the Boltzmann constant, T the absolute temperature, η_o the solvent viscosity, and D_o the diffusion coefficient at infinite dilution. The hydrodynamic radius is the sum of the core radius R_c and the corona thickness L. R_c can be calculated from the aggregation number, N_{agg}, through the eq 2 valid for a dry core.

$$\frac{4}{3}\pi R_c^{\,3} = \frac{N_{agg}.N_{P2VP}m}{\rho N_{av}} \quad (2)$$

where m and ρ are the molecular weight and the density of the vinylpyridine units and N_{av} is the Avogadro number. R_c was found to be 12.3 nm, and the corona thickness L is calculated to 24.7 nm. The R_H/R_g ratio is 0.7, which is very close to the theoretical value of 0.775 predicted for hard spheres.[10] Therefore, spherical mi-

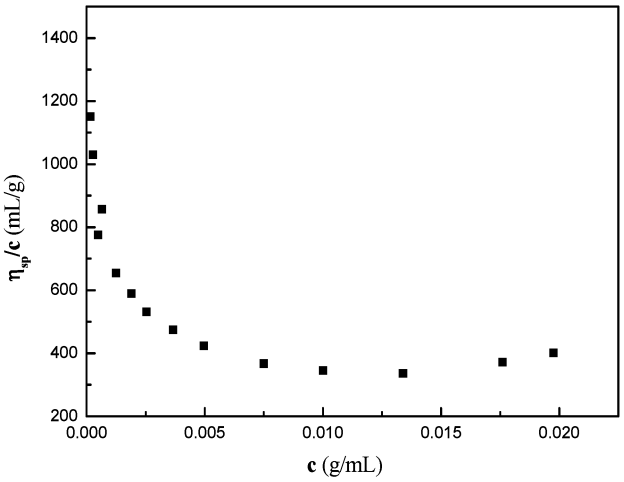

Figure 7. Concentration dependence of $(Kc/\Delta I)_{\Theta=0}$ for $PAA_{134}-P2VP_{628}-PAA_{134}$ in water at the high pH region at 25 °C.

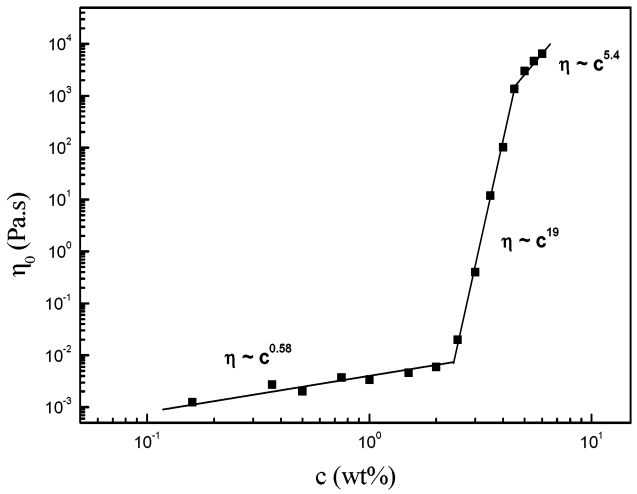

Figure 8. Double logarithmic plot of the zero shear viscosity, η_o as a function of concentration for the $PAA_{134}-P2VP_{628}-PAA_{134}$ in water at pH 3.4 and 25 °C.

celles are likely to be formed with the corona chains stretched 73% of the fully stretched conformation of the PAA blocks ($L = 134 \times 0.25 = 33.5$ nm).

The Low pH Region. In the low pH region, the copolymer behaves as a polyampholyte. Static light scattering experiments in dilute aqueous solutions gives an apparent molecular weight 6.2×10^4 g mol^{-1} close to the value calculated from the degree of polymerization of the precursor copolymer determined in THF (Table 1), revealing that the copolymer is molecularly dissolved. Moreover, a polyelectrolyte behavior is exhibited at pH 3.4, as shown by the viscosimetric results in Figure 7, where the reduced viscosity is plotted vs concentration. This behavior is attributed to the positive charges of the protonated pyridine groups (see also Figure 3).

The interest is focused on the behavior of the system close to pH 3.4 where a maximum in reduced viscosity has been observed (Figure 5). In more concentrated solutions, a physical gel is formed. Steady-state shear viscosity measurements were performed in order to characterize the rheological behavior. At concentrations below 2.5 wt %, the shear viscosity is independent of shear rate, exhibiting a Newtonian behavior. At higher concentrations, the shear rate dependent viscosity profile reveals three distinct regimes. A Newtonian plateau is first observed followed by a remarkable shear-thickening effect. The viscosity passes through a maximum and an abrupt shear-thinning behavior is finally exhibited. Details of the rheological behavior of the system will appear in a forthcoming paper.[11]

In Figure 8, the zero-shear viscosity is plotted as a function of c. Three concentration regimes can be distinguished: (a) $c < c_g$, where the viscosity η_o is on the order of that of the water and increases smoothly with c. The exponent of the power law is 0.58. The critical gel concentration is determined at $c_g = 2.4$ wt %. Beyond this concentration, a fast increase of the viscosity is evidenced. The viscosity enhancement follows a scaling low with a very high exponent close to 19. This law is valid until a certain concentration c' beyond which the rate of viscosity increase diminishes as the scaling exponent decreases to 5.4. c' distinguishes the second from the third regime. However, the physical meaning of c' cannot yet be elucidated.

The concentration dependent viscosity behavior of the present system has been observed also in telechelic nonionic associative polymers[12] and is predicted by the "flower" model of Semenov et al.[13] This model mainly concerns flexible chains end-capped with hydrophobic blocks, which differs entirely from the polymer under investigation. Although $PAA_{134}-P2VP_{628}-PAA_{135}$ can be considered as telechelic since it is composed of a long central P2VP block end-capped with shorter PAA blocks, the ionic nature of both blocks and the association mode does not permit any correlation between the two polymeric systems. However, it seems that physical gelation can be described qualitatively by this model irrespective of the association mechanism.

The first region below c_g is characterized by a scaling law $\eta_o \sim c^{0.58}$. With pH close to 3.4, the middle P2VP chain has been mostly protonated and behaves as a polyelectrolyte (Figure 7). The scaling theory for polyelectrolytes gives an exponent 0.5 in the unentangled semidilute regime[14] and this is close to what is observed in the present system. It seems that in this concentration regime the behavior of the system is governed mainly by the polyelectrolytic character of the longer middle block. Above c_g the viscosity rises very sharply with a power law $\eta_o \sim c$.[19] The exponent in the semidilute entangled regime is theoretically predicted to be 1.5,[14] much lower than that found by us. Therefore, the first crossover concentration c_g clearly is not the entanglement concentration but a percolation threshold beyond of which a three-dimensional transient network is formed through intermolecular association. The nature of the interactions is of course not hydrophobic as in conventional associative polymers but rather electrostatic. In the pH range where the physical gel is formed, P2VP is mostly ionic bearing positive charges while PAA is mainly in its acidic form. However the existence of some negative charges due to the dissociation of the acrylic acid units cannot be excluded. Moreover, as it has been found a portion of pyridine rings is protonated by the presence of PAA since the heat of P2VP protonation exceeds considerably the corresponding values in the absence of PAA. This was attributed to a cooperative transfer of the proton from the PAA carboxyl group to the pyridine ring.[15]

Therefore, it is reasonable to assume that the physical cross-links of the network arise mainly from intermolecular association between the negatively charged PAA segments located in the end blocks and the positively

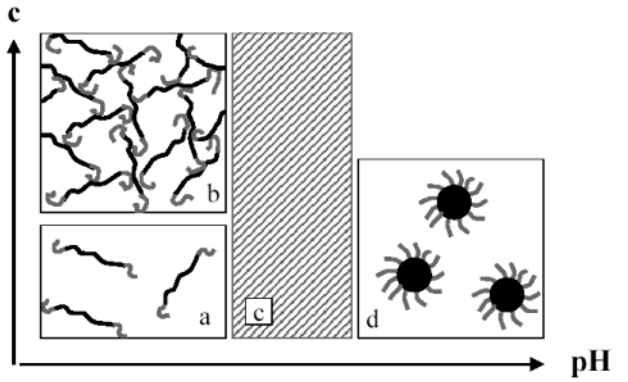

Figure 9. Schematic representation of the phase behavior of the $PAA_{134}-P2VP_{628}-PAA_{134}$ aqueous solutions as a function of pH: (a) molecular dissolution; (b) transient network; (c) precipitation region; (d) compact micelles.

charged segments located in the middle block (see schematics in Figure 9). Stabilization of this kind of complexation by hydrogen bonding from the PAA units is likely to occur. To confirm the electrostatic nature of the association mechanism, solutions of 3.5 wt % polymer were prepared in 0.5 and 1 M NaCl and explored by rheological measurements. Indeed a dramatic drop of the viscosity was observed with increasing ionic strength due to the screening effect of the electrostatic interactions between the oppositely charged segments. It should be mentioned here that association between block copolymers of poly(2-vinylpyridine)-*b*-poly(ethylene oxide) and poly(methacrylic acid)-*b*-poly(ethylene oxide) through interpolyelectrolyte complexation has been observed in the range $2 < pH < 6$ although the effective p*K* of the poly(methacrylic acid) is higher than that of PAA.[16]

Conclusions

A well-defined asymmetric polyampholyte with a long P2VP central block end-capped with relative short PAA blocks was synthesized by anionic polymerization and investigated in aqueous solutions as a function of pH.

A rich phase behavior was observed as it is demonstrated schematically in Figure 9. Three distinct pH regions can be distinguished. At low pH region ($pH < 4$) and at low concentrations, the polymer is molecularly dissolved and the electrostatic character of the protonated P2VP middle block governs its behavior. Beyond a percolation threshold and in a limited pH range, a three-dimensional physical network is formed through electrostatic interactions. At intermediate pH values and around the isoelectric point, the polymer is precipitated. Finally at the high pH region, regular micelles are formed composed of P2VP hydrophobic compact cores surrounded by extended charged PAA chains. The phase behavior of the block polyampholyte is reversible.

To the best of our knowledge, it appears for the first time that a water-soluble polymer may be self-organized reversibly into two distinct and completely different structures (i.e., from a transient three-dimensional network to compact micelles) by changing the pH of the aqueous media. This interesting and novel behavior is due to the nature and the specific architecture of the polymer named asymmetric triblock polyampholyte. Diblock polyampholytes of the same nature (P2VP−PAA) self-assemble leading to the formation of spherical micelles only in the high pH region.[17] The present polymeric species could be considered as a good paradigm for a multifunctional polymer.

Further work is in progress in order to explore the influence of the various molecular characteristics (e.g., molecular weight, composition) on the aqueous solution properties, as well as to explore new combinations of other amphoteric polymer constituents keeping the same architecture.

Acknowledgment. This work was supported by the Operational Program for Education and Initial Vocational Training on Polymer Science and Technology of the University of Patras, through the Ministry of Education and Religious Affairs in Greece.

References and Notes

(1) Procházka, K.; Martin, T. J.; Munk, P.; Webber, S. E. *Macromolecules* **1996**, *29*, 6518.
(2) Martin, T. J.; Procházka, K.; Munk, P.; Webber, S. E. *Macromolecules* **1996**, *29*, 6071.
(3) Gohy, J-. F.; Antoun, S.; Jerôme, R. *Macromolecules* **2001**, *34*, 7435.
(4) (a) Kamachi, M.; Kurihara, M.; Stille, J. K. *Macromolecules* **1972**, *5*, 161. (b) Kurihara, M.; Kamachi, M.; Stille, J. K. *J. Polym. Sci., Chem. Ed.* **1973**, *11*, 587.
(5) (a) Baines, F. L.; Armes, S. P.; Billingham, N. C.; Tuzar, Z. *Macromolecules* **1998**, *29*, 8151. (b) Lowe, A.B.; Billingham, N. C.; Armes, S. P. *Macromolecules* **1998**, *31*, 5991. (c) Varoqui, R.; Tran, Q.; Pefferkorn, E. *Macromolecules* **1979**, *12*, 831. (d) Morishima, Y.; Hashimoto, T.; Itoh, Y.; Kamachi, M.; Nozakura, S. I. *J. Polym. Sci., Polym. Chem.* **1982**, *20*, 299. (e) Bekturov, E. A.; Frolova, V. A.; Kudaibergenov, S. E.; Schulz, R. C.; Zoller, J. *Macromol. Chem.* **1990**, *191*, 457. (f) Becturov, E. A.; Kudaibergenov, S. E.; Khamzamulina, R. E.; Frolova, V. A.; Nurgalieva, D. E.; Schulz, R. C.; Zoller, J. *Macromol. Chem. Rapid Commun.* **1992**, *13*, 225. (g) Goloub, T.; de Keizer, A.; Cohen Stuart, M. A. *Macromolecules* **1999**, *32*, 8441. (h) Butun, N.; Lowe, A. B.; Billingham, N. C.; Armes, S. P. *J. Am. Chem. Soc.* **1999**, *121*, 4288. (i) Hadjikallis, G.; Hadjiyannakou, S. C.; Vamvakaki, M.; Patrickios, C. S. *Polymer* **2002**, *43*, 7269. (j) Liu, S.; Armes, S. P. *Angew. Chem., Int. Ed.* **2002**, *41*, 1413. (k) Creutz, S.; van Stam, J.; Antoun, S.; de Schryver, F. C.; Jerôme, R. *Macromolecules* **1977**, *30*, 4078. (l) Gohy, J.-F.; Creutz, S.; Garcia, M.; Mahltig, B.; Stamm, M.; Jerôme, R. *Macromolecules* **2000**, *33*, 6378.
(6) (a) Patrickios, C. S.; Hertler, W.R.; Abbott, N. L.; Hatton, T. A. *Macromolecules* **1994**, *27*, 930. (b) Chen, W.-Y.; Alexandridis, P.; Su, C.-K.; Patrickios, C. S.; Hertler, W. R.; Hatton, T. A. *Macromolecules* **1995**, *28*, 8604. (c) Patrickios, C. S.; Lowe, A. B.; Armes, S. P.; Billingham, N. C. *J. Polym. Sci., Polym. Chem.* **1998**, *36*, 617. (d) Giebeler, E. Stadler, R. *Macromol. Chem. Phys.* **1997**, *1385*, 198. (e) Bieringer, R.; Abetz, V.; Müller, A. H. E. *Eur. Phys. J. E.* **2001**, *5*, 5.
(7) (a) Rayt, R.; Forte, R.; Jacobs, C.; Jérôme, R.; Ouhadi, T.; Teyssié Ph,; Varshney, S. R. *Macromolecules* **1987**, *20*, 1442. (b) Klein, J. W.; Lamps, J.-P.; Gnanou, Y.; Rempp, P. *Polymer* **1991**, *32*, 2278.
(8) (a) Alfrey, T. J.; Morawetz, H. *J. Am. Chem. Soc.* **1952**, *74*, 436. (b) Alfrey, T. J.; Fuoss, R. M.; Morawetz, H.; Pinner, H. *J. Am. Chem. Soc.* **1952**, *74*, 438.
(9) Patrickios, C. S. *J. Colloid Interface Sci.* **1995**, *175*, 256.
(10) Yamakawa, H. *Modern Theory of Polymer Solutions;* Harpar and Row: New York, 1971.
(11) Bossard, F.; Sfika, V.; Tsitsilianis, C. Manuscript in preparation.
(12) Francois, J.; Maitre, S.; Rawiso, M.; Sarazin, D.; Beinert, G.; Isel, F. *Colloids Surf. A.* **1996**, *112*, 251.
(13) Semenov, A. N.; Joanny, J.-F.; Khokhlov, A. R. *Macromolecules* **1995**, *28*, 1066.
(14) Dobrynin, A. V.; Colby, R. H.; Rubinstein, M. *Macromolecules* **1995**, *28*, 1859.
(15) Topchieva, I. N.; Beshir, A.; Kabanov, V. A. *Vysokomol. Soedin.* **1971**, *13*, 396.
(16) Gohy, J.-F.; Varshney, S. K.; Jerôme, R. *Macromolecules* **2001**, *34*, 3361.
(17) Briggs, N. P.; Budd, P. M.; Price, C.; Robb, I. D. *Eur. Polym. J.* **1992**, *28*, 739.

MA0300084